31st Annual International Conference of the IEEE EMBS
Minneapolis, Minnesota, USA, September 2-6, 2009

Visualization and Segmentation of Liver Tumors Using Dynamic Contrast MRI

Ashish Raj and Krishna Juluru

Abstract— Hepatocellular carcinoma (liver tumor) is one of the most common malignancies causing an estimated one million deaths annually, and the fastest growing form of cancer in the United States. Dynamic Contrast Enhanced MRI (DCE-MRI) is a useful way to characterize tumor response to contrast agent uptake, but the method still lacks maturity in terms of quantifying tumor burden and viability. We propose a semi-supervised technique for visualizing and measuring liver tumor burden and viability from DCE-MRI examinations. In order to solve the challenging segmentation problem, we exploit prior information about the spatio-temporal characteristics of DCE-MRI data, and perform k-means clustering in a hybrid intensity-spatial feature space.

I. Introduction

Hepatocellular carcinoma or HCC (liver tumor) is one of the most common malignancies causing an estimated one million deaths annually, and the fastest growing form of cancer in the United States. Depending on the extent of tumor burden, adjuvant therapy in nonsurgical patients and surgically eligible patients awaiting transplant include transarterial chemoembolization (TACE), percutaneous ethanol injection (PEI), radiofrequency ablation (RFA), microwave coagulation therapy (MCT), and laser induced thermotherapy (LITT)[1]. Current standards for measuring treatment response in oncology include the *Response Evaluation Criteria in Solid Tumors (RECIST)* [2] and *WHO Criteria.* The difficulty with these standards is that they assess tumor response in only two states, either successfully treated or unsuccessfully treated. Furthermore, as both of these criteria are based on purely anatomic measures, they fail to take into account that not all "lesions" are equivalent vis-à-vis viability. A recent study using size criteria, and subjective assessment of new tumors, found that CT and MR have an overall sensitivity and specificity of 35% and 64%, respectively, in detection of presence of residual HCC following TACE [3].

An accurate evaluation of liver tumor viability must take into account three factors: size, metabolism (potentially measured by MR diffusion characteristics and/or MR spectroscopy), and vascular perfusion (potentially measured by MR contrast enhancement)[4]. Determining tumor extent, growth and response to therapy is essential for both clinical trials and routine clinical practice, but quantitative strategies are currently limited. Minimally invasive imaging-derived biomarkers can greatly aid early detection, characterization and measurement of progression of liver tumors, and assessment of response to therapy. However, quantitative biomarkers from imaging techniques like dynamic contrast-enhanced MRI (DCE-MRI) have had limited impact due to significant variability in anatomic site, pathologic condition, physiologic features of the normal and pathologic cells and their microenvironment. CT Perfusion studies by Sahani et al. correlated parameters of blood flow (BF), blood volume (BV), mean transit time (MTT), and permeability surface area product (PS) with presence of tumor and stage of tumor[6]. BF and MTT showed statistically significant correlations with presence of tumor, and all parameters showed statistically significant correlations with tumor grade. Earlier studies measured global perfusion of the liver in terms of a mean Hepatic Perfusion Index (HPI)[7], which is neither locally specific not informative enough for staging purposes. Perfusion modeling has shed considerable light on the pharmacokinetics of contrast uptake in carcinomas[9], but this wealth of information has not been effectively combined into quantitative biomarkers related to tumor location, extent and growth.

It is notoriously difficult to estimate the parameters of a multi-exponential perfusion model from a small number of noisy, unreliable time points. Our insight is that these challenges can only be overcome by fully exploiting prior information about the spatio-temporal characteristics of DCE-MRI data. We propose a semi-supervised technique for visualizing DCE properties of tissues; segmenting liver volumes into normal tissue, vasculature, enhancing carcinomas and necrotic tumors; and measuring liver tumor burden and viability from DCE-MRI examinations. The classification will rely on dynamic contrast response of various tissue types as well as on spatio-temporal image priors to obtain anatomically realistic segmentations. A distinguishing feature of this proposal is the use of pathology-proven gold standard for validation purposes, in keeping with our goal of establishing conformity to clinically established standard. Experimental data were acquired at 3 Tesla with **Gadoxetate Disodium (**Eovist®**),** a new liver-specific contrast agent having greater hepatic uptake and up to 50% excretion through the liver[15].

Manuscript received April 23 2009
Authors are with Radiology, Cornell Weill Medical College, New York.

II. METHOD

Dynamic Feature Extraction from DCE-MRI data

In DCE-MRI, the subject is injected with a contrast agent which appears hyperintense in a T1-weghted MRI scan. The contrast is injected a few seconds after the scan has been started, in order to first obtain a baseline or pre-contrast MRI. Then after the contrast bolus has had a chance to run through the vasculature, several time points are acquired. When MRI signal from a given voxel are plotted, the time-course of the contrast, as it perfuses through the tissue, can be readily characterized. Let us denote by v_p a voxel in the volume indexed by the set of voxels $p \in \mathcal{P}$, and the associated time series $x_p(n)$ where n indexes the time points in the DCE-MRI exam. The total number of voxels in the volume is denoted by $|\mathcal{P}|$. A typical plot of $x_p(n)$ in the case of rabbit liver enhancement using Gadoxetate Disodium is shown in figure 1. Different tissue classes have varying response to contrast agent – healthy tissue in general enhances less than enhancing carcinomas, but more than necrotic tissue, which does not enhance appreciably.

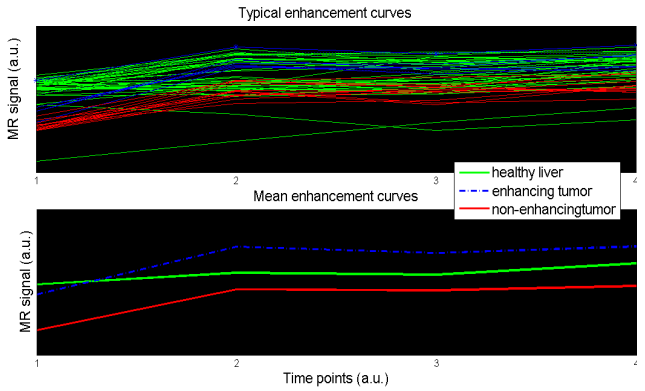

Figure 1: Typical plot of time-resolved MR signal of various tissue classes before (1st time point) and after injection of contrast agent Gadoxetate Disodium.

In this paper, the following *dynamic features* from the time-resolved signal are extracted, as depicted in figure 2: baseline (pre-contrast) MR signal (BL), peak enhancement (PE), and area under the enhancement curve (AUC). At the coarse time-scale shown in Figure 2(a), more detailed dynamic features that are routinely extracted from vascular perfusion studies at much higher temporal resolution (figure 2(b)) are not available. We show both models here for illustration – in our work we use both models, depending on the availability of high temporal resolution data.

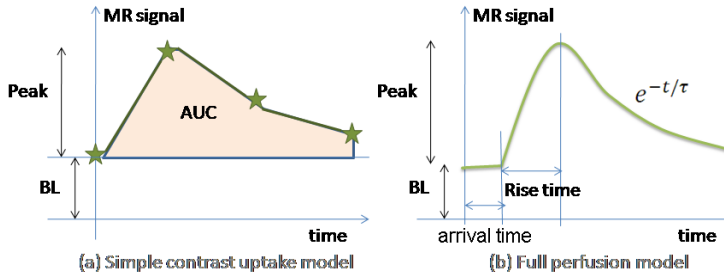

Figure 2: Schematic of contrast uptake in liver tissue, (a) a simple model, and (b) full perfusion model. When few time points are available, it is more appropriate to use model (a).

The three low-resolution features, when mapped in pseudocolor onto RGB color space, are shown in figure 3, and conveys the power of feature-space mapping of DCE-MRI data – just as a color picture conveys additional information compared to a black-and-white image, the feature-space mapped image conveys additional information that is simply not available in any single MRI image.

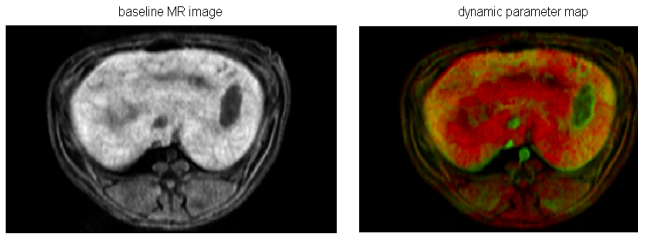

Figure 3: RGB of feature space extracted from DCE-MRI

Mathematically, we denote the single voxel time series as vector $\mathbf{x}_p = \{x_p(n) \mid n \in [1, N]\}$ and the entire time-resolved volume as the set of single-voxel signals $\mathbf{X} = \{\mathbf{x}_p \mid p \in \mathcal{P}\}$. Let the corresponding temporal feature vector be $\boldsymbol{\theta}_p = \{\theta_p(f) \mid f \in \mathcal{F}\}$, where each f represents a temporal response feature from the parameter set $\mathcal{F} = \{BL, PE, AUC\}$ as in figure 2 above. Later we will add more perfusion features to $\mathcal{F}$, depending on the time resolution available - like mean transit time (MTT), rise time and decay rate of wash-out phase (τ).

The MR volume contains several tissue regions with differing temporal response characteristics. We will denote the different tissue classes by membership to the *label set*

$$\mathcal{L} = \{normal\ liver, enhancing\ tumor, nonenhancing\ tumor, vasculature\}$$

and the number of tissue types as set cardinality $|\mathcal{L}|$.

We assume that time-response models are available for each tissue class, e.g. piecewise linear models[9]. Denote these dynamic models by model functions $\mathcal{T}_1 \ldots \mathcal{T}_{|\mathcal{L}|}$, such that the time series at a voxel of tissue class l is given by $\mathbf{x}_p = \mathcal{T}_l(\boldsymbol{\theta}_p)$

Each model relates the unknown perfusion parameters – e.g. MTT, τ, PE, BLetc – to the time series at the voxel.

By denoting the set of these models a $\mathcal{T} = \{\mathcal{T}_1 \dots \mathcal{T}_{|\mathcal{L}|}\}$s and the set of all temporal features as $\boldsymbol{\Theta} = \{\boldsymbol{\theta}(p)|p \in \mathcal{P}\}$, the relationship between the observed time series data and temporal parameters can be conveniently expressed as

$$\mathbf{X} = \mathcal{T}(\boldsymbol{\Theta})$$

The above feature-space mapping is a powerful way to visualize the time-resolved data, because various tissue classes appear much better discriminated than in the original MR images, from any single time point. However, the feature space construct is also a rich source of data for the purpose of tissue classification and segmentation.

Tissue Classification and Segmentation of Time-Resolved DCE-MRI Data

Tissue segmentation from MRI modalities[10,11,12] is a mature field now, and several good tools exist in the community. However, these tools work on 3D spatial but non-time-resolved data, and are therefore unable to exploit the additional benefits provided by time-resolved data. Methods that do work on time-resolved data employ simple clustering algorithms along with supervised seed growing[10] which require significant user input and can be erroneous in presence of inhomogeneity or local texture. On the other hand, several approaches to analyzing 1D time-resolved signals were reported, notably in MR perfusion[9,11,13]. It has been shown, much like our feature map above, that various dynamic perfusion parameter maps provide important information regarding the dynamic response of tissue. Although most of these methods were developed for brain imaging, some have successfully been adapted for use in more general cancer imaging scenarios[11]. Voxel-by-voxel classification can certainly be performed using standard k-means clustering techniques[14] but this is problematic in presence of noise and lack of temporal resolution.

Mathematically the classification task can be formalized as the mapping of the 4D feature-space volume $\boldsymbol{\Theta}$ onto the tissue label set $\mathcal{L}$

$$\mathcal{C} : \boldsymbol{\Theta} \longrightarrow \mathcal{L}^{|\mathcal{P}|}$$

such that $\mathcal{C}(p) \triangleq \mathcal{C}(\boldsymbol{\theta}_p)$ represents the tissue class label assigned to the p-th voxel.

The segmentation algorithm finds the class labeling which satisfies two orthogonal constraints:

1. For each voxel p, its class label $\mathcal{C}(p)$ must be equal, as far as possible, to the label predicted by a simple independent voxel-wise k-means classifier[14].
2. The set of all labels for the image must respect known tissue boundaries and be spatially contiguous.

The reason for the second constraint is that in the presence of noise and other artifacts, the single-voxel estimate of tissue class can be unreliable, and additional spatial constraints can help to regularize the process. To achieve this, we perform the following classification task. Define the augmented feature vector at each voxel p as

$$\bar{\boldsymbol{\theta}}_p = \begin{bmatrix} \boldsymbol{\theta}_p \\ xcoord_p \\ ycoord_p \\ zcoord_p \end{bmatrix}$$

A k-means nearest neighbor classifier is used to cluster the set of feature space $\boldsymbol{\Theta}$ into $|\mathcal{L}|$ classes, by minimizing the ratio of intra-cluster distances to inter-cluster distances[14]. Note that without the augmentation described above, the normal voxel-wise classifier would result; augmentation provides the classifier with additional *spatial* features which help in satisfying constraints (2). Consequently, our algorithm is less sensitive to noise, and produces more contiguous regions with smoother tissue boundaries. Note also the complete absence of isolated regions of falsely labels tissue.

A comprehensive software suite was written in MATLAB to implement the above segmentation scheme. This software is currently being tested and evaluated on the Rabbit HCC data. A screenshot illustrating the software's functionality is shown in figure 4. The software has the following modules:

i) *Semi-supervised Liver Segmentation Module*: User is presented with a series of axial scans of the 3D volume, and asked to place a small number of boundary points to help the software to segment the liver volume. This procedure was necessitated by the difficulty of completely unsupervised automatic liver segmentation, which sometimes failed. It not necessary to manually draw ROIs around the liver. A small number of user-input points in the perimeter of the liver in a small number of slices is sufficient to accurately delineate the liver mass.

ii) *Time-series analysis*: The voxels contained within the segmented liver volume are then passed to the time-domain analysis module, which returns feature-space quantities as described above. A full classification and segmentation is then performed on this data using the augmented feature-vector approach above, and the detected clusters are presented to the user in color maps.

iii) *Semi-supervised tumor segmentation*: We implemented instead a semi-supervised approach, whereby 4-way segmentation is first performed on the liver mass, and the user is then asked to click on detected tumor regions. Again, this does not involve laborious manual drawing of ROIs around the tumors; the user simply selects tumor regions by clicking within the appropriate detected segments.

iv) *3-way tumor segmentation module*: The segmented tumor regions are then refined with morphological filters to remove boundary inconsistencies, holes and erroneous isolated voxels. The resulting regions are then processed using the same time-resolved feature clustering method used in ii)

above, but this time using the 3 classes of interest – normal liver, enhancing tumor, non-enhancing necrotic tumor. Since the manual intervention has already removed the sources of error described in iii), this module is completely automatic.

v) ***Biomarkers***: Finally, the total volumes of both enhancing and non-enhancing tumor regions are computed, and computer-aided viability and tumor burden scores are presented as per

$$\text{tumor burden} = \text{total volume of enhancing} + \text{nonenhancing tumors}$$

$$\text{computed viability} = \frac{\text{volume of enhancing tumors}}{\text{total volume of enhancing} + \text{nonenhancing tumors}} \times 100$$

Perfusion-related quantities can now be reported separately for each tissue class

$$\{\text{mean} - \text{enhancement}_l, \quad \text{mean} - \tau_l, \quad \text{mean} - \text{risetime}_l\} \text{ for all } l \in \mathcal{L}$$

III. RESULTS

Significant preliminary work has been completed in our lab towards a new segmentation-based scheme for obtaining volumetric biomarkers of HCC. Our method was developed and tested on data from a pre-existing study at Johns Hopkins University involving hepatocellular carcinoma (HCC) grown in a Rabbit model[4]. Rabbit models of HCC have been shown to demonstrate a physiology similar to that of humans[4]. The above DCE-MRI data was obtained as part of a previous IRB approved study to assess MR diffusion characteristics of HCC before and after TACE. The DCE-MRI exams were obtained using a standard T_1-weighted MR acquisition sequence, with the following timed phases: pre-contrast phase (0s), arterial phase (20s), portal-venous phase (60) and delayed phase (120s). Tumor size and degree of necrosis was determined through pathologic dissection in all animals. Dissections were performed by pathologists under guidelines and techniques that ensure accurate and reproducible measurement of tumor size and degree of necrosis, and this pathology data served as the gold standard. A novel liver-specific Gadolinium-based contrast agent Gadoxetate Disodium (Eovist®) was intravenously injected.

A typical visualization and segmentation result from Rabbit data are shown in figure 4. Note the performance of the method at various stages of operation, from initial clustering to final segmentation of tumors. At this stage fully validated quantitative data are not available. However, a preliminary evaluation of tumor volumes and overlap with pathology data indicate a **Pearson correlation of 85%**. This is considered relatively good agreement by radiologists, given the vast differences in pathology and MR imaging approaches.

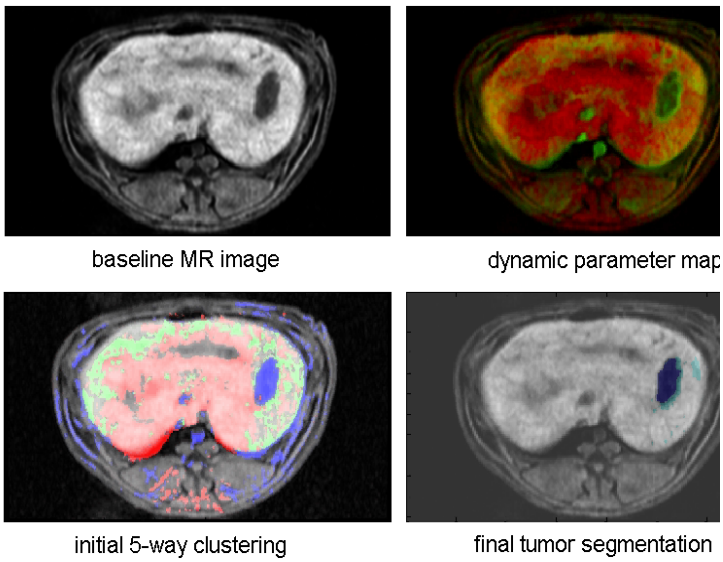

Figure 4: screenshot of HCC software functionality

IV. DISCUSSION AND FUTURE WORK

Our software must be significantly expanded and modified before it becomes useful for human clinical applications:

i) ***Extension to higher temporal resolution data***: current HCC data have only 4 time points – 1 pre-contrast and 3 post-contrast, with a time window of 2 minutes. This is clearly inadequate for accurate characterization of dynamic response of liver tissue, which is known to have a wash-in / wash-out duration exceeding several minutes.

ii) We will investigate ***autoregressive (AR) and AR+moving average (ARMA) time-domain models***[16,17], which can provide parametric features independent of vascular perfusion models and might be useful for clustering purposes. Our methods are agnostic to the pharmacokinetics of a particular contrast agent as well as to the choice of the temporal response model, whether MR perfusion models or AR/ARMA, or any other model.

iii) ***Removing the need for user input***: Inherent variability of signal and intensity within liver tissue, presence of vascular as well as tumor tissue, instrumentation noise, motion and other artifacts, etc necessitated our semi-syupervised approach, but they can be overcome with additional effort and result in a completely automated segmentation algorithm. We can exploit tissue gradients and the difference in dynamic response, which we believe will be adequate for a suitable clustering algorithm to reliably perform the segmentation.

Finally, our methods need to be validated on high-resolution human data, which will be acquired at Cornell Medical Center (New York, NY). For this purpose we will have access to both a retrospective human dataset as well as a proposed prospective MR study on human subjects recruited

from HCC patients at our hospital who are slated to undergo TACE treatment. We will correlate our computed results with the clinical outcomes already recorded as metadata within patients' records, including clinical outcome scores, survival times and serological liver function tests (e.g. Billirubin, ALT and AST). These will be used in pairwise Pearson correlation analysis against our computed biomarkers. In addition, conventional radiologist readings under both RECIST and EASL-modified WHO criteria will be tabulated for all subjects and correlated against our results.

REFERENCES

[1] Gu T, Li CX, Feng Y, Wang Q, Li CH, Li CF. Trans-arterial gene therapy for hepatocellular carcinoma in a rabbit model. World J Gastroenterol 2007; 13:2113-2117.

[2] Therasse P, Arbuck SG, Eisenhauer EA, et al. New guidelines to evaluate the response to treatment in solid tumors. European Organization for Research and Treatment of Cancer, National Cancer Institute of the United States, National Cancer Institute of Canada. J Natl Cancer Inst 2000; 92:205-216

[3] Hunt SJ, Yu W, Weintraub J, Prince MR, Kothary N. Radiological Monitoring of Hepatocellular Carcinoma Tumor Viability after Transhepatic Arterial Chemoembolization: Estimating the Accuracy of Contrast-enhanced Cross-sectional Imaging with Histopathologic Correlation. J Vasc Interv Radiol 2009; 20:30-38

[4] Kamel IR, Bluemke DA, Ramsey D, et al. Role of diffusion-weighted imaging in estimating tumor necrosis after chemoembolization of hepatocellular carcinoma. AJR Am J Roentgenol 2003; 181:708-710

[5] Zhao B, Schwartz LH, Larson SM. Imaging Surrogates of Tumor Response to Therapy: Anatomic and Functional Biomarkers. J Nucl Med 2009; 50:239-249

[6] Sahani DV, Holalkere NS, Mueller PR, Zhu AX. Advanced hepatocellular carcinoma: CT perfusion of liver and tumor tissue--initial experience. Radiology 2007; 243:736-743.

[7] White MJ, O'Gorman RL, Charles-Edwards EM, et al. Parametric mapping of the hepatic perfusion index with gadolinium-enhanced volumetric MRI. Br J Radiol 2007; 80:113-120.

[8] Totman JJ, O'Gorman R L, Kane PA, Karani JB. Comparison of the hepatic perfusion index measured with gadolinium-enhanced volumetric MRI in controls and in patients with colorectal cancer. Br J Radiol 2005; 78:105-109.

[9] Yamashita Y, Baba T, Baba Y, Nishimura R, Ikeda S, Takahashi M, Ohtake H, Okamur H. Dynamic Contrast-enhanced MR Imaging of Uterine Cervical Cancer: Pharmacokinetic Analysis with Histopathologic Correlation and Its Importance in Predicting the Outcome of Radiation Therapy. Radiollogy 2000; 216(3): 803-809

[10] Liang Z, Macfall JR, Harrington DP. Parameter estimation and tissue segmentation from multispectral MR images. IEEE Trans Med Imaging. IEEE Transactions on Medical Imaging 1994;13(3):441-9.

[11] Chong VF, Zhou JY, Khoo JB, Huang J, LimTK. Nasopharyngeal Carcinoma Tumor Volume Measurement. *Radiology* 2004;231:914-921.

[12] Kaus MR, Warfield SK, Nabavi A, Black PM, Jolesz FA, Kikinis R. Automated Segmentation of MR Images of Brain Tumors. *Radiology* 2001;218:586-591.

[13] Murase K, Yamazaki Y, Shinohara M. Autoregressive Moving Average (ARMA) Model Applied to Quantification of Cerebral Blood Flow Using Dynamic Susceptibility Contrast-enhanced Magnetic Resonance Imaging. Magnetic Resonance in Medical Sciences 2003;2(2): 85-95.

[14] Hartigan JA, Wong MA. A K-Means Clustering Algorithm. Applied Statistics 1979 28 (1): 100–108.

[15] Website: http://pharma.bayer.com/scripts/pages/en/news_room/news_room/news_room62.php

[16] Liang G, Wilkes DM, The Recursive Linear Identification Method for ARMA Model Estimation, Proceedings IEEE, 1992, pp 677-682

[17] Smith MR, Nichols ST, Henkelman RM, Wood ML. Application of Autoregressive Moving Average Parametric Modeling in Magnetic Resonance Image Reconstruction. IEEE Transactions on Medical Imaging 1986; 5(3): 132-139